

Online Decoupled Stator and Rotor Resistances Adaptation for Speed Sensorless Induction Motor Drives by a Time Division Approach

Jiahao Chen, Jin Huang

Abstract—The paper addresses the method for stator and rotor resistance identification in speed sensorless induction motor drives. The instability problem caused by pure integration of the voltage model of rotor flux is handled by introducing correction terms in voltage model. It is, however, shown that the third-order persistent excitation condition for simultaneous identification of stator, rotor resistances and rotor speed can barely be satisfied even with extra excitations in rotor flux modulus command. And an adaptive observer which is not persistently excited may become instable when exposed to bounded disturbances. Hence to design a robust flux observer, concept of time division multiplexing is incorporated into the observer design. That is, stator resistance is identified as the flux modulus is flat, while rotor resistance is adapted as a ramp flux modulus command is applied. This relaxes persistent excitation condition to order two, and as a drawback, the ramp flux modulus command incurs speed ripples. The decoupled identifiability of stator resistance is designed and explained, a rigorous input-to-state stability analysis of both the mismatch (between voltage model and current model) and the error (between actual rotor flux and current model) is set forth, and a convergence analysis of parameters is elaborated. To validate the feasibility, simulation and experiment results are included in the text as well.

Index Terms—adaptive observers, induction motors, input-to-state stability, parameter estimation, persistency of excitation, speed sensorless drives

NOMENCLATURE

L_s, L_r, L_m	Stator, rotor and magnetizing inductances.
σ	Leakage coefficient $\sigma = 1 - L_m^2/(L_s L_r)$.
r_s, r_r	Stator and rotor resistances respectively.
τ_r, α	Rotor time constant $\tau_r = L_r/r_r$, and its reciprocal $\alpha = 1/\tau_r$.
n_{pp}, p	n_{pp} is the number of the pole pairs, while $p = \frac{d}{dt}$ is the differential operator.
T_L, J_s	Load torque and shaft moment of inertia respectively.
u_s, i_s, ψ_r	Vectors of voltages, currents and rotor fluxes in $\alpha\beta$ frame, where $u_s = [u_{\alpha s}, u_{\beta s}]^T$, $i_s = [i_{\alpha s}, i_{\beta s}]^T$, $\psi_r = [\psi_{\alpha r}, \psi_{\beta r}]^T$.
*	An aster * stands for values used in the controller.
$\hat{\cdot}$	A hat $\hat{\cdot}$ designates estimated values in the observer.
VM, CM	Abbreviations for voltage model and current model.

J. Chen and J. Huang are with the College of Electrical Engineering, Zhejiang University, Hangzhou 310027, China (e-mail: horychen@qq.com; ee_huangj@emb.zju.edu.cn).

$\hat{\psi}_r^{VM}, \hat{\psi}_r^{CM}$ Estimated values of rotor fluxes from voltage model and current model respectively, where $\hat{\psi}_r^{VM} = [\hat{\psi}_{\alpha r}^{VM}, \hat{\psi}_{\beta r}^{VM}]^T$, and $\hat{\psi}_r^{CM} = [\hat{\psi}_{\alpha r}^{CM}, \hat{\psi}_{\beta r}^{CM}]^T$.

\hat{i}_r Estimated rotor currents $\hat{i}_r \triangleq L_r^{-1}(\hat{\psi}_r^{CM} - L_m i_s)$.

ε Mismatch between voltage model and current model, $\varepsilon = [\varepsilon_\alpha, \varepsilon_\beta]^T \triangleq \hat{\psi}_r^{VM} - \hat{\psi}_r^{CM}$.

e Error between the actual rotor flux and that of current model, $e = [e_\alpha, e_\beta]^T \triangleq \psi_r - \hat{\psi}_r^{CM}$.

MT A superscript MT stands for the $M-T$ frame whose M -axis is aligned along the estimated rotor flux vector $\hat{\psi}_r^{CM}$, and T -axis is 90° leading to M -axis.

T is the transform matrix from $\alpha\beta$ frame to $M-T$ frame defined in (16), e.g. $T\hat{\psi}_r^{CM} = \hat{\psi}_r^{CM MT} = [\hat{\psi}_{Mr}^{CM}, \hat{\psi}_{Tr}^{CM}]^T$. A superscript T means transpose.

$\omega_r, \omega_{\psi_r}$ Electrical rotor speed, and the rotatory speed of the $M-T$ frame respectively.

\sim A tilde \sim denotes error values that deviate from actual values.

$\tilde{r}_s, \tilde{\alpha}, \tilde{\omega}_r$ Errors for estimated stator resistance, estimated reciprocal of rotor time constant, and estimated rotor speed respectively, where $\tilde{r}_s = r_s - \hat{r}_s$, $\tilde{\alpha} = \alpha - \hat{\alpha}$, and $\tilde{\omega}_r = \omega_r - \hat{\omega}_r$.

$\hat{\theta}, \tilde{\theta}$ $\hat{\theta}$ is the estimated vector of estimated parameters defined in (8), and $\tilde{\theta} = \theta - \hat{\theta}$.

Φ Regressive matrix defined in (8).
 Γ Gain matrix of adaptation, $\Gamma = \text{diag}(\gamma_1, \gamma_2, \gamma_3)$, where γ_1 and γ_2 are designed with variable structures as in (19).

v^{VM}, v^{CM} Correction terms for VM and CM defined in (19), which are functions of ε and of $\text{sgn}(e_T)$.

I, J $I = \begin{bmatrix} 1 & 0 \\ 0 & 1 \end{bmatrix}$, $J = \begin{bmatrix} 0 & -1 \\ 1 & 0 \end{bmatrix}$.

I. INTRODUCTION

IT is well known that indirect field orientated control is sensitive to rotor resistance changes [1], whereas direct field oriented control is inherently insensitive with rotor resistance variations [2]. However, in speed sensorless applications, the accuracy of estimated speed is deteriorated by detuned rotor resistance regardless of control strategies. Besides, stator resistance is crucial in low speed operation, and poor

knowledge of stator resistance even leads to instability of observers [3]. Thereupon, the adaptivity to both stator and rotor resistance is required in speed sensorless field oriented control drives. In this paper, adaptive observers are concerned, and other methods such as extended Kalman filter and artificial neural networks are well reviewed in [4], [5]. Those techniques are of good performance but also require more expensive microprocessors. In the sequel, the adaptive observers are classified by different drives in adaptation rules:

- (1) Full order observers. The estimated current error and the estimated flux error are needed for parameter update in theory.
- (2) Current observers. The drive is the estimated current error.
- (3) Flux observers. The mismatch between voltage and current model of rotor flux is exploited to tune parameters.

1) *Full order observers*: The full order observer is proposed by Kubota et al [6] and [7], which acquires the estimated error of full states to tune parameters, i.e. the estimated error of (stator) currents and the estimated error of (rotor) fluxes. However the latter is unknown. Simply neglecting the estimated error of fluxes leads to instability problem during regeneration [8]. Thus, lots of remedies are proposed. A compensation term is added in the speed adaptation by Tajima et al [9], whereas only limited stability margin is obtained. Stability of speed estimation over the whole operation can be recovered by proper design of observer feedback gain and adaptation law [10]. Stability analysis of speed and stator resistance estimations are further conducted in [11]. However, the simultaneous identifiability of r_s , τ_r and ω_r is not yet discussed.

To identify rotor resistance, an extra low frequency component of flux modulus command is usually excited [6], [7], [9], accounting for the fact that rotor time constant and rotor speed can not be distinguished at steady state where the modulus of the rotor flux is constant [12], [13].

However, torque pulsation exists due to the extra sinusoidal flux modulus command. Thus, a method for identification of rotor resistance and rotor speed at transient is proposed [14]. But this becomes impractical in the case where the thermal variation of rotor resistance happens at steady state.

2) *Current observers*: the estimated error of fluxes is treated as parameters with known dynamics to be identified by Marino et al [15] and [16], [17], so that only the estimated error of currents is acquired in adaptation rules. As a matter of fact, there are two main consequent deficiencies: i) integrals of currents have to be introduced which is unrealistic since biased measurement may occur; ii) with r_s of uncertainty, it leads to coupling between unknown parameters like $r_s r_r$ and $r_s \omega_r$, which incurs high order observers (up to order 11) and rather complicated persistent excitation conditions.

Those aforementioned shortcomings are overcome a decade later by Marino et al [18], [19], in which the time scale separation proposed by Jadot et al [20] and [21] is adopted. The authors isolate r_s identification under the *a priori* knowledge of slow variation of r_s , which relaxes the persistent excitation conditions. And it is indicated that under specific observability and identifiability conditions, solutions

to simultaneous identification of r_s , τ_r and ω_r do exist locally. The scheme is competitive since dynamic nonlinear control is incorporated, so that the pulsation of torque caused by an extra sinusoidal command of rotor flux modulus is somewhat decreased. The detailed proofs can be found in [22]. However, the convergence analysis of the adaptive observer dynamics holds only locally, i.e. uncertainty in \hat{r}_s is assumed to be sufficiently small. Furthermore, only the identifiability in first approximation of the stator resistance at steady state is assured, and in order to derive correspondences between persistent excitation conditions and motor operations, the accurate value of stator resistance has to be assumed known in the first place in [19].

3) *Flux observers*: As is known to all, there are two simple models for rotor fluxes estimation, namely the voltage model (VM) and the current model (CM). And the mismatch between those two models can be put to tune the estimated rotor speed [23], [2]. Stator resistance identification is further included in [24], [25], where the authors adopt the phraseology of “interchange of the roles between reference and adjustable models to identify r_s and ω_r ”. It should be indicated, when there are uncertainties in both \hat{r}_s and $\hat{\omega}_r$, neither of the estimated fluxes from VM nor from CM can be regarded as the actual rotor fluxes anymore. But in [24], the flux mismatch between VM and CM is used to drive adaptation rules, while the stability analysis is still performed for the estimated errors from actual rotor fluxes.

In practice, the instability of the pure integration of VM is a common problem among those papers dealing with flux observers, and lots of techniques are proposed to cope with it. In [23], [2], [24], high-pass filter is added at the output of VM, which however, causes undesired amplitude gain and phase shift. Those amplitude gain and phase shift can be compensated according to [26], which however, is merely valid at steady state. In [27], with an extra adaptive mechanism designed for proper compensation, dynamic compensation is achieved. On the other hand, it is possible to avoid the pure integration of VM, and for instance, the derivative of flux mismatch can be used to tune parameters [25].

In this paper, an adaptive flux observer which employs the flux mismatch ε to identify r_s , τ_r and ω_r is presented. The adaptive observer does not resort to time scale separation, instead it is inspired by the concept of time division multiplexing. That is, r_s and ω_r are identified during constant rotor flux modulus, while τ_r and ω_r are identified during varying rotor flux modulus. And instead of injecting an extra sinusoidal flux modulus command, the more efficient ramp flux modulus command is adopted. However, speed ripples exist as the ramp flux modulus command is applied, which is deemed to be a deficiency of the scheme. Flux estimate is achieved as well, and computation burden is decreased¹. Such an observer is of order 7 and incredibly simple, since only a variable structure in the basic adaptation rules is needed.

During stability analysis, no assumption of known resistances is made, and the resistance not in adaptation is treated

¹Tajima et al [2] uses another stand-alone observer to estimate fluxes since the pure integration of VM is replaced by a low-pass filter

as disturbance. Thus, input-to-state stability analysis is needed, and is performed to the mismatch ε as well as the error e . Moreover, a convergence analysis is conducted to parameters, and it is shown that $\tilde{\alpha}$ and $\tilde{\omega}_r$ converge to zero after \tilde{r}_s does. By the concept of input-to-state stability, explicit correspondences between persistent excitation conditions and motor operations can be concluded even with stator resistance of uncertainty.

As a feature, correction terms (which are functions of ε) are proposed to reject disturbances and to stabilize pure integration of VM, in virtue of the fact that the mismatch ε is available to compute. Thus none of those preceding techniques for solving the problem of pure integration of VM is needed. Besides, the complete decoupled identifiability of stator resistance acquires sliding mode terms in correction terms.

II. TIME DIVISION DECOUPLED ADAPTATION OF RESISTANCES

A. Mathematic Models

1) *Models for Control:* The symmetric and non-saturated induction motor dynamics in α - β frame are described by the fifth-order nonlinear state space equations (1)

$$L_s \sigma p i_s = u_s - r_s i_s - L_m L_r^{-1} p \psi_r \quad (1a)$$

$$p \psi_r = \alpha L_m i_s - \alpha \psi_r + \omega_r J \psi_r \quad (1b)$$

$$J_s n_{pp}^{-1} p \omega_r = n_{pp} L_m L_r^{-1} (i_s^T J \psi_r) - T_L \quad (1c)$$

From (1b), the following formulae are derived in M - T frame

$$i_{Ms}^* = \alpha^{-1} L_m^{-1} p \psi_{Mr}^* + L_m^{-1} \psi_{Mr}^* \quad (2)$$

$$\omega_{sl}^* = \alpha L_m i_{Ts}^* \psi_{Mr}^{*-1} \neq \alpha i_{Ts}^* i_{Ms}^{*-1} \quad (3)$$

where the derivative of the flux modulus command $p \psi_{Mr}^*$ is included in M -axis current command generator (2), to make sure that a ramp flux command can be tracked; and (3) is used to compute slip frequency ω_{sl}^* . It is worth mentioning that using of $\omega_{sl}^* = \alpha i_{Ts}^* i_{Ms}^{*-1}$ may cause drastic speed ripples during fluxes varying. Torque current command i_{Ts}^* is generated by the speed Proportional-Integral (PI) regulator to resist unknown load torque of low frequencies. In addition, i_{Ts}^* can be exploited to detect the sign of the T -axis flux error e_T [28].

2) *Models for Observation:* The voltage model (4a) and the current model (4b) of rotor flux in α - β frame [2] are given by

$$p \psi_r = L_r L_m^{-1} (u_s - r_s i_s) - \sigma L_s L_r L_m^{-1} p i_s \quad (4a)$$

$$p \psi_r = -\alpha (\psi_r - L_m i_s) + \omega_r J \psi_r \quad (4b)$$

B. Elementary Observer Design

Observers for VM and CM in α - β frame are

$$p \hat{\psi}_r^{VM} = L_r L_m^{-1} (-\hat{r}_s i_s - L_s \sigma p i_s + u_s) + v^{VM} \quad (5a)$$

$$p \hat{\psi}_r^{CM} = -\hat{\alpha} (\hat{\psi}_r^{CM} - L_m i_s) + \hat{\omega}_r J \hat{\psi}_r^{CM} + v^{CM} \quad (5b)$$

in which a hat $\hat{\cdot}$ designates estimated value; v^{VM} and v^{CM} are correction terms yet to be designed. The parameter updating laws are

$$\begin{cases} p \hat{r}_s = \gamma_1^{-1} (L_r L_m^{-1} i_{\alpha s} \varepsilon_\alpha + L_r L_m^{-1} i_{\beta s} \varepsilon_\beta) \\ p \hat{\alpha} = \gamma_2^{-1} [-(\psi_{\alpha r}^{CM} - L_m i_{\alpha s}) \varepsilon_\alpha - (\psi_{\beta r}^{CM} - L_m i_{\beta s}) \varepsilon_\beta] \\ p \hat{\omega}_r = \gamma_3^{-1} (-\psi_{\beta r}^{CM} \varepsilon_\alpha + \psi_{\alpha r}^{CM} \varepsilon_\beta) \end{cases} \quad (6)$$

where $\varepsilon = \hat{\psi}_r^{VM} - \hat{\psi}_r^{CM}$ is the mismatch between VM's and CM's outputs. The equivalent matrix form of (6) follows

$$\dot{\hat{\theta}} = \Gamma^{-1} \Phi^T \varepsilon \quad (7)$$

where $\Gamma^{-1} = \text{diag}(\gamma_1^{-1}, \gamma_2^{-1}, \gamma_3^{-1})$ is the gain matrix, Φ the regressive matrix, $\hat{\theta}$ the vector of estimated parameters

$$\Phi = \begin{bmatrix} L_r L_m^{-1} i_{\alpha s} & -(\hat{\psi}_{\alpha r}^{CM} - L_m i_{\alpha s}) & -\hat{\psi}_{\beta r}^{CM} \\ L_r L_m^{-1} i_{\beta s} & -(\hat{\psi}_{\beta r}^{CM} - L_m i_{\beta s}) & \hat{\psi}_{\alpha r}^{CM} \end{bmatrix} \quad (8)$$

$$\hat{\theta} = [\hat{r}_s \quad \hat{\alpha} \quad \hat{\omega}_r]^T$$

C. Identifiability of Resistances and Speed

The simultaneous identifiability of r_s , α and ω_r can be sufficiently (but not necessarily) determined by the positive definiteness of the matrix Θ

$$\Theta \triangleq \Phi^T \Phi = \begin{bmatrix} L_r^2 L_m^{-2} i_s \cdot i_s & -L_r^2 L_m^{-1} i_s \cdot \hat{i}_r & L_r L_m^{-1} \hat{\psi}_r^{CM} \times i_s \\ & L_r^2 \hat{i}_r \cdot \hat{i}_r & L_r \hat{i}_r \times \hat{\psi}_r^{CM} \\ (\text{Sym.}) & & \hat{\psi}_r^{CM} \cdot \hat{\psi}_r^{CM} \end{bmatrix} \quad (9)$$

where $\hat{i}_r \triangleq L_r^{-1} (\hat{\psi}_r^{CM} - L_m i_s)$; a dot ' \cdot ' means dot product (defined by $a \cdot b = a^T b$) and a cross ' \times ' means cross product (defined by $a \times b = -a^T J b$). The determinate of Θ is

$$|\Theta| = \frac{L_r^4}{L_m^2} (i_s \cdot i_s) (\hat{i}_r \cdot \hat{i}_r) (\hat{\psi}_r^{CM} \cdot \hat{\psi}_r^{CM}) \left\{ 1 - \cos^2 \langle i_s, \hat{i}_r \rangle \right. \\ \left. - \sin^2 \langle \hat{i}_r, \hat{\psi}_r^{CM} \rangle - \frac{L_r^2}{L_m^2} \frac{(\hat{i}_r \cdot \hat{i}_r)}{(i_s \cdot i_s)} \sin^2 \langle \hat{i}_r, \hat{\psi}_r^{CM} \rangle \right. \\ \left. - 2 \sqrt{\frac{(\hat{i}_r \cdot \hat{i}_r)}{(i_s \cdot i_s)}} \cos \langle i_s, \hat{i}_r \rangle \sin^2 \langle \hat{i}_r, \hat{\psi}_r^{CM} \rangle L_r L_m^{-1} \right\} \quad (10)$$

where $\langle \cdot, \cdot \rangle$ denotes the angle between two vectors. It is observed that $|\Theta| < 0$ when $\langle \hat{i}_r, \hat{\psi}_r^{CM} \rangle = 90^\circ$ (namely $\hat{i}_{Mr} = 0$); And even with nonzero \hat{i}_{Mr} , it is barely possible to give positive results of $|\Theta|$ under regular motor operations. By Sylvester's criterion, the positive definiteness of Θ can not be established, i.e. the persistent excitation (PE) condition that $\Phi^T \Phi$ is positive definite does not hold.

In the remainder of the text, the requirement is relaxed to identify only two of r_s , α and ω_r at a time. We compute

some minors of Θ to illustrate the identifiability between two parameters

$$M_{33} = \frac{L_r^4}{L_m^2} \left[(i_s \cdot i_s) (\hat{i}_r \cdot \hat{i}_r) - (i_s \cdot \hat{i}_r)^2 \right] \quad (11a)$$

$$M_{22} = \frac{L_r^2}{L_m^2} \left[(i_s \cdot i_s) (\hat{\psi}_r^{CM} \cdot \hat{\psi}_r^{CM}) - (\hat{\psi}_r^{CM} \times i_s)^2 \right] \quad (11b)$$

$$M_{11} = L_r^2 \left[(\hat{i}_r \cdot \hat{i}_r) (\hat{\psi}_r^{CM} \cdot \hat{\psi}_r^{CM}) - (\hat{i}_r \times \hat{\psi}_r^{CM})^2 \right] \quad (11c)$$

where M_{ij} denotes the minor of the entry in the i -th row and j -th column; and it's observed that the simultaneous identifiability is achieved between

$$r_s \& \alpha, \quad \text{if } M_{33} > 0, \quad \text{i.e. } \cos^2 \langle i_s, \hat{i}_r \rangle \neq 1 \quad (12a)$$

$$r_s \& \omega_r, \quad \text{if } M_{22} > 0, \quad \text{i.e. } \sin^2 \langle \hat{\psi}_r^{CM}, i_s \rangle \neq 1 \quad (12b)$$

$$\alpha \& \omega_r, \quad \text{if } M_{11} > 0, \quad \text{i.e. } \sin^2 \langle \hat{i}_r, \hat{\psi}_r^{CM} \rangle \neq 1 \quad (12c)$$

where it's worth mentioning that (12a) is sufficed by nonzero i_{Tr} (acceleration or nonzero T_L), (12b) is trivially satisfied, and (12c) is achieved by nonzero \hat{i}_{Mr} (varying rotor flux modulus). The above conclusions are consistent with the more general results obtained in [12] and [13], and to be specific, the PE condition that satisfied by nonzero second derivatives of speed is excluded here.

D. Proposed Scheme

An adaptive observer that does not satisfies PE conditions is probably unstable to bounded disturbance [29]. This fact along with the unavailable simultaneous identifiability of r_s , α and ω_r motivates that we update only two parameters at a time, and treat the uncertainty in the third one as disturbance. Obviously this idea does not usually work, because the asymptotical stability of the adaptive observer may be lost due to the existence of disturbance, and parameters may not converge to actual values. Fortunately, the decoupled identifiability of r_s with respect to $\tilde{\alpha}$ and $\tilde{\omega}_r$ exists when the mismatch ε and the error e are limited to zero. And in theory, sliding mode terms are needed in the T -axis of the dynamics to limit ε_T and e_T to zero. In this sub-section, we first take an insight into this decoupled identifiability and make a proposition about it, and then conduct stability analysis.

1) *Decoupled Identifiability of r_s :* Introduce estimated errors \hat{r}_s , $\tilde{\alpha}$, $\tilde{\omega}_r$

$$\begin{aligned} \hat{r}_s &= r_s - \tilde{r}_s \\ \hat{\alpha} &= \alpha - \tilde{\alpha} \\ \hat{\omega}_r &= \omega_r - \tilde{\omega}_r \end{aligned} \quad (13)$$

Substituting (13) in (5) to eliminate estimated terms, we rewrite the observer equations as

$$\begin{aligned} p\hat{\psi}_r^{VM} &= \underbrace{L_r L_m^{-1} (-r_s i_s - L_s \sigma p i_s + u_s)}_{\text{equal to } p\psi_r \text{ in (4a)}} + L_r L_m^{-1} \tilde{r}_s i_s + v^{VM} \\ p\hat{\psi}_r^{CM} &= \underbrace{-\alpha (\psi_r - L_m i_s) + \omega_r J \psi_r}_{\text{equal to } p\psi_r \text{ in (4b)}} + \tilde{\alpha} (\hat{\psi}_r^{CM} - L_m i_s) \\ &\quad - \tilde{\omega}_r J \hat{\psi}_r^{CM} + v^{CM} + \alpha e - \omega_r J e \end{aligned} \quad (14)$$

where the error $e = \psi_r - \hat{\psi}_r^{CM}$ is unknown; the two under-bracketed terms on the right are actually equal, thus the mismatch dynamics (15) are derived

$$\dot{\varepsilon} = (v^{VM} - v^{CM}) - (\alpha I - \omega_r J) e + \Phi \tilde{\theta} \quad (15)$$

where the mismatch $\varepsilon = \hat{\psi}_r^{VM} - \hat{\psi}_r^{CM}$ is known. Introduce the gyrate transform matrix T

$$T = \frac{1}{\sqrt{\hat{\psi}_{\alpha r}^{CM} + \hat{\psi}_{\beta r}^{CM}}} \begin{bmatrix} \hat{\psi}_{\alpha r}^{CM} & \hat{\psi}_{\beta r}^{CM} \\ -\hat{\psi}_{\beta r}^{CM} & \hat{\psi}_{\alpha r}^{CM} \end{bmatrix} \quad (16)$$

Pre-multiplying the mismatch dynamics (15) by transform matrix T from (16) yields

$$\dot{\varepsilon}^{MT} = v^{VM\,MT} - v^{CM\,MT} - (\alpha I - \omega_r J) e^{MT} + T \Phi \tilde{\theta} - \omega_{\psi_r} J \varepsilon^{MT} \quad (17)$$

Assume that ε and e had converged to 0 and notice that $v^{VM}|_{\varepsilon=e=0} = v^{CM}|_{\varepsilon=e=0} = 0$, then the dynamics (17) became

$$\begin{aligned} 0 &= T \Phi \tilde{\theta} \\ &= \begin{bmatrix} L_r L_m^{-1} i_{Ms} & -(\hat{\psi}_{Mr}^{CM} - L_m i_{Ms}) & -\hat{\psi}_{Tr}^{CM} \\ L_r L_m^{-1} i_{Ts} & -(\hat{\psi}_{Tr}^{CM} - L_m i_{Ts}) & \hat{\psi}_{Mr}^{CM} \end{bmatrix} \begin{bmatrix} \tilde{r}_s \\ \tilde{\alpha} \\ \tilde{\omega}_r \end{bmatrix} \end{aligned} \quad (18)$$

from which noticing that $\hat{\psi}_{Tr}^{CM} \equiv 0$, we discover that

- 1) $\tilde{\omega}_r$ is always biased due to nonzero $\tilde{\alpha}$ or nonzero \tilde{r}_s , if $i_{Ts} \neq 0$;
- 2) we have $\tilde{r}_s = 0$, if $\hat{i}_{Mr} \triangleq L_r^{-1} (\hat{\psi}_{Mr}^{CM} - L_m i_{Ms}) = 0$;
- 3) further in the case of $\tilde{r}_s = 0$ and $\hat{i}_{Mr} \neq 0$, estimations of α and ω_r end unbiased.

To sum up, we give the following outcome.

Proposition 1—Time Division Decoupled Adaptation (T-DDA): To make the flux observer given in (5) robust to perturbation and adaptive to r_s , α and ω_r , we propose a variable structure in the flux modulus command, correction terms in (5) and adaptation gains in (6)

$$\begin{aligned} \text{flat struct.} &\quad \begin{cases} |\psi_r^*| = \text{Const.} \\ v^{VM\,MT} = -k^{VM} \varepsilon^{MT} + f^{VM\,MT} - f^{CM\,MT} \\ v^{CM\,MT} = -f^{CM\,MT} \\ \text{diag}(\gamma_1^{-1}, \gamma_2^{-1}, \gamma_3^{-1}) = \text{diag}(\gamma_{rs}, 0, \gamma_{\omega r}) \end{cases} \\ \text{ramp struct.} &\quad \begin{cases} \frac{d}{dt} |\psi_r^*| = \text{Const.} \\ v^{CM\,MT} = 0 \\ v^{VM\,MT} = -k^{VM} \varepsilon^{MT} \\ \text{diag}(\gamma_1^{-1}, \gamma_2^{-1}, \gamma_3^{-1}) = \text{diag}(0, \gamma_\alpha, \gamma_{\omega r}) \end{cases} \end{aligned} \quad (19)$$

where

$$f^{VM\,MT} = - \begin{bmatrix} 0 \\ c_1 \text{sgn}(\varepsilon_T) \end{bmatrix}, \quad f^{CM\,MT} = - \begin{bmatrix} 0 \\ c_2 \text{sgn}(e_T) \end{bmatrix}$$

are sliding mode terms, c_1 and c_2 are the magnitudes of the sign function, $v^{VM\,MT} = T v^{VM}$, $v^{CM\,MT} = T v^{CM}$, T is defined in (16), and k^{VM} , γ_{rs} , γ_α and $\gamma_{\omega r}$ are proper constants; by 'ramp structure' it means constant $\frac{d}{dt} |\psi_r^*|$ where the PE condition (12c) is sufficed and $\hat{\alpha}$ begins to adapt; and by 'flat structure' it means a constant $|\psi_r^*|$ where \hat{r}_s begins to update.

In the proposition, e_T in $f^{CM\,MT}$ is unknown, though it is possible to get the sign of e_T by detecting the changes in torque current command i_{Ts}^* when a short duration pulse is injected in the magnetizing current command i_{Ms}^* [28], since $e_T \neq 0$ is equivalent to biased field orientation.

2) *Stability Analysis:* The stability analysis for TDDA is twofold according to different structures in (19). This subsection is going to show that i) in flat structure, ε , e , \tilde{r}_s and $\tilde{\omega}_r$ are stable exposed to $\tilde{\alpha}$; and ii) in ramp structure, ε , e , $\tilde{\alpha}$ and $\tilde{\omega}_r$ are stable exposed to \tilde{r}_s .

Subtracting (5b) from (4b), the dynamics of e are deduced in M - T frame

$$\begin{aligned}\dot{e}^{MT} = & -(\alpha I - \omega_r J)e^{MT} - v^{CM\,MT} \\ & + \begin{bmatrix} -L_r \hat{i}_r^{MT} & J\hat{\psi}_r^{CM\,MT} \end{bmatrix} \begin{bmatrix} \tilde{\alpha} \\ \tilde{\omega}_r \end{bmatrix} - \omega_{\psi r} J e^{MT}\end{aligned}\quad (20)$$

We firstly focus on the system in flat structure. To be concise, the dynamics (17) and (20) are rewritten into

$$\dot{x} = Ax + B^f z^f + C^f w^f + v^f \quad (21)$$

where a symbol substitution is taken by defining

$$\begin{aligned}A &= \begin{bmatrix} -k^{VM} I - \omega_{\psi r} J & -(\alpha I - \omega_r J) \\ 0 & -(\alpha I - \omega_r J) - \omega_{\psi r} J \end{bmatrix}, \\ B^f &= \begin{bmatrix} L_r L_m^{-1} \hat{i}_s^{MT} & J\hat{\psi}_r^{CM\,MT} \\ 0 & J\hat{\psi}_r^{CM\,MT} \end{bmatrix}, \quad C^f = \begin{bmatrix} -L_r \hat{i}_r^{MT} \\ -L_r \hat{i}_r^{MT} \end{bmatrix}, \\ x &= \begin{bmatrix} \varepsilon^{MT} \\ e^{MT} \end{bmatrix}, \quad z^f = \begin{bmatrix} \tilde{r}_s \\ \tilde{\omega}_r \end{bmatrix}, \quad w^f = \tilde{\alpha}, \quad v^f = \begin{bmatrix} f^{VM\,MT} \\ f^{CM\,MT} \end{bmatrix}\end{aligned}$$

where superscript f denotes ‘flat structure’; x designates the state, z^f the parameter estimated error, w^f the disturbance and v^f is for disturbance rejecting. And by noticing that $\Phi^T \varepsilon = \Phi^T T^{-1} T \varepsilon = (T\Phi)^T \varepsilon^{MT}$, the 1st and 3rd equations of the updating laws (6) yield dynamics of z^f

$$\dot{z}^f = -\text{diag}(\gamma_1^{-1}, \gamma_3^{-1}) \begin{bmatrix} L_r L_m^{-1} \hat{i}_s^{MT} & J\hat{\psi}_r^{CM\,MT} \end{bmatrix}^T \varepsilon^{MT} \quad (22)$$

It is easy to show that $B^f T B^f$ is positive definite if the PE condition (12b) is satisfied. And if $B^f T B^f$ is positive definite, the input-to-state stability of x and z^f is a direct result from the Extended Persistency of Excitation Lemma given by Marino et al [29] by choosing a Lyapunov function candidate $V : \mathbb{R}^4 \times \mathbb{R}^2 \rightarrow \mathbb{R}$

$$V(x, z^f) = \frac{1}{2} x^T x + \frac{1}{2} z^f \text{diag}(\gamma_1, \gamma_3) z^f \quad (23)$$

whose derivative along (21) and (22) follows

$$\begin{aligned}\dot{V} = & x^T A x + x^T \underbrace{\left(\begin{bmatrix} 0 \\ J\hat{\psi}_r^{CM\,MT} \end{bmatrix} \tilde{\omega}_r + C^f w^f + v^f \right)}_{\text{regarded as disturbance } w_{eq}^f} \quad (24) \\ \leq & x^T A x + \frac{\varrho}{2} \|x^T\|^2 + \frac{1}{2\varrho} \|w_{eq}^f\|^2 \leq -\delta_1 \|x\|^2 + \delta_2 \|w_{eq}^f\|^2\end{aligned}$$

where it is possible to find a scalar $\delta_1 > 0$ if ϱ is chosen sufficiently small, and the scalar $\delta_2 \geq \frac{1}{2\varrho}$.

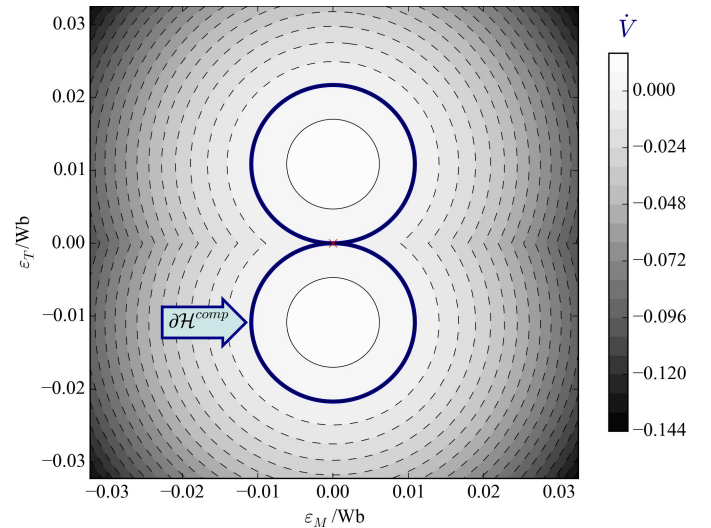


Fig. 1. Contour of \dot{V} with respect to ε^{MT} and sketch of the boundary of the positive invariant set $\mathcal{H}^{\text{comp}}$ when $c_1 = c_2 = 0$, e^{MT} is assumed to be 0, and $(k^{VM} + \hat{\alpha})^{-1} L_r \hat{i}_{Tr} \tilde{\alpha} = \mp 0.019215$, where $k^{VM} + \hat{\alpha} = 100$, $L_r = 0.4826$ H, $\hat{i}_{Tr} = -3$ A, $\tilde{\alpha} = \pm 1.5$ Hz.

Similar procedure can be proceeded for the system in ramp structure, which may be rewritten in

$$\dot{x} = Ax + B^r z^r + C^r w^r \quad (25)$$

where superscript r designates ‘ramp structure’; the corresponding matrices B^r , C^r , the parameter estimated error z^r and the disturbance w^r are defined by

$$\begin{aligned}B^r &= \begin{bmatrix} -L_r \hat{i}_r^{MT} & J\hat{\psi}_r^{CM\,MT} \\ -L_r \hat{i}_r^{MT} & J\hat{\psi}_r^{CM\,MT} \end{bmatrix} = \begin{bmatrix} I \\ I \end{bmatrix} \begin{bmatrix} -L_r \hat{i}_r^{MT} \\ J\hat{\psi}_r^{CM\,MT} \end{bmatrix}^T \\ C^r &= \begin{bmatrix} L_r L_m^{-1} \hat{i}_s^{MT} \\ 0 \end{bmatrix}, \quad z^r = \begin{bmatrix} \tilde{\alpha} \\ \tilde{\omega}_r \end{bmatrix}, \quad w^r = \tilde{r}_s\end{aligned}$$

If $B^r T B^r$ is positive definite, which is equivalent to the nonzero \hat{i}_{Mr} condition (12c), then x and z^r is input-to-state stable (ISS) [29].

Based on the conclusions above and the convergence analysis in the Appendix A, we have the following results.

- R1 The system (x, z^f) in flat structure is ISS with respect to $\tilde{\alpha}$, if the PE condition (12b) is sufficed.
- R2 The system (x, z^r) in ramp structure is ISS with respect to \tilde{r}_s , if the PE condition (12c) is sufficed.
- R3 $\tilde{r}_s \rightarrow 0$ as $t \rightarrow \infty$ in flat structure even when $\tilde{\omega}_r \neq 0$ and $\tilde{\alpha} \neq 0$, if $c_1 > |L_r \hat{i}_{Tr} \tilde{\alpha}|$ and $c_2 > |\hat{\psi}_{Mr}^{CM} \tilde{\omega}_r - L_r \hat{i}_{Tr} \tilde{\alpha}|$.
- R4 $[\tilde{\alpha} \quad \tilde{\omega}_r] \rightarrow 0$ as $t \rightarrow \infty$, if $\tilde{r}_s = 0$.
- R5 Flux estimate is achieved, i.e. $\hat{\psi}_r^{CM} \rightarrow \psi_r$, $t \rightarrow \infty$.

Remark: If c_1 and c_2 are designed to 0 in the flat structure, the input-to-state stability of the system is not lost. Consider a set $\mathcal{H} = \{x | \dot{V} < 0\}$. The trajectory of ε^{MT} and e^{MT} in \mathcal{H} would behave as if the origin was asymptotically stable, and it will eventually enter the positive invariant set $\mathcal{H}^{\text{comp}} = \mathbb{R}^4 \setminus \mathcal{H}$ and be trapped there. For example, in the case of $e^{MT} = 0$, the boundary $\partial\mathcal{H}^{\text{comp}}$ is shaped like a ‘∞’ depicted in ε_M - ε_T

TABLE I
MOTOR DATA

Parameter	Notation	Values
Rated power	—	4 kW
Rated speed	—	1440 rpm
Rated voltage	—	380 V, Y-connect
Rated current	—	8.8 A
Number of pole pairs	n_{pp}	2
Stator resistance	r_s	3.04 Ω
Rotor resistance	r_r	1.69 Ω
Stator inductance	L_s	0.4826 H
Rotor inductance	L_r	0.4826 H
Magnetizing inductance	L_m	0.47 H
Shaft inertia	J_s	0.01 kg · m ²

TABLE II
COEFFICIENT USED IN CONTROL

Parameter	Notation	Values
Correction gain of VM	k^{VM}	100
Adaptation gain of speed	$\gamma_{\omega r}$	5e3
Adapt. gain of stator resistance	γ_{rs}	5
Adapt. gain of inverse rotor time const.	γ_α	800
Magnitudes of switching terms	c_1, c_2	0, 0
Slope of ramp command	k_{slope}	0.5 Wb/s
Duration of flat structure	t_{DoF}	6 s
Duration of ramp structure	t_{DoR}	0.4 s
Duty ratio of r_s adaptation	ϑ_{duty}	50%
Rotor flux modulus command	$ \psi_r^* $	0.6 ~ 0.8 Wb

plane (see Fig. 1), and the diameter of the circles equals to $(k^{VM} + \hat{\alpha})^{-1} \|L_r \hat{i}_{Tr}\| \|\tilde{\alpha}\|$. Thus, $\|\varepsilon\|$ can be arbitrary small by choosing a sufficiently large k^{VM} .

E. Brief Summary

At this point, the design is complete. The seventh-order adaptive observer is given in (5) and (6). The correction terms v^{VM} and v^{CM} are designed in (19). The adaptive gains with variable structure are given in (19).

The whole scheme is dependent on L_s , L_r , L_m and the initial values of \hat{r}_s , \hat{r}_r and $\hat{\omega}_r$; it contains 9 design parameters (i.e., k^{VM} , γ_{rs} , γ_α , $\gamma_{\omega r}$, c_1 , c_2 , slope of ramp command k_{slope} , duration of flat structure t_{DoF} and duration of the ramp structure t_{DoR}); its inputs are u_s and i_s ; its outputs are \hat{r}_s , $\hat{\alpha}$, $\hat{\omega}_r$ and observed rotor flux $\hat{\psi}_r^{VM}$ or $\hat{\psi}_r^{CM}$. A block diagram of the scheme is sketched in Fig. 2a.

III. VALIDATION STUDIES

A. System Setup

The whole scheme is implemented in the digital signal processor TMS320F28335. The sampling frequency is 8 kHz. A three phase, squirrel-cage induction motor is driven by a voltage-source inverter. The carrier frequency of sinusoidal pulse width modulation (SPWM) is 4 kHz. The motor is coupled with a separately excited DC generator, thus the load torque is proportional to rotor speed, and the load torque is indicated by a constant factor K_{DC} times the DC generator armature current i_{Load} . Sensed currents and the reconstructed voltages are used for observation and control. An optical encoder is equipped for verification use. Fig. 2b sketches the

block diagram of the speed sensorless indirect field orientation control system. The numerical values of the tested motor, and the coefficients designed for control are listed in Table I and Table II respectively. The rotor flux modulus command is sufficiently below the rated value, so that the saturation problem is avoided. And the coefficients of the PI current regulator are $K_p^{cur.} = 12$, $T_i^{cur.} = 0.05$; and the coefficients of the PI speed regulator are $K_p^{speed} = 0.5$, $T_i^{speed} = 0.08$.

B. Simulation Results

To make sense out of the proposition, a illustrative simulation is conducted. The motor model (1) is simulated using the Runge-Kutta method. The sampling time of simulation is 1e-4 second. The waveforms of $L_m i_{Ms}^*$, $|\hat{\psi}_r^{CM}|$, \hat{r}_s , $\hat{\alpha}$, $\hat{\omega}_r$, ω_r , $i_{\alpha s}$ and electromagnetic torque T_{em} are presented in Fig. 3. The speed command is set to 50 rpm and the load torque is given by 6 Nm.

From Fig. 3, the values of \hat{r}_s and $\hat{\alpha}$ are accurate at the beginning, and step to 60% of the actual values at $t = 15$ s. The estimated speed $\hat{\omega}_r$ is always kept at 50 rpm, whereas the actual speed ω_r deviates. The adaptation of resistances is turned on at $t = 30$ s. \hat{r}_s adapts in flat structure where $|\hat{\psi}_r^*|$ is constant, while $\hat{\alpha}$ is updated in ramp structure where $|\hat{\psi}_r^*|$ is varying. $\hat{\alpha}$ may be detuned (jumps to 140.5% at $t = 32$ s) before \hat{r}_s converges, and tends to actual value ultimately. The actual speed ω_r approaches back to 50 rpm, as the resistances converge.

Nevertheless, the ramp flux command imposes negative effects on motor performance. T_{em} is perturbed during ramp structure, which causes speed ripples. The magnitude of the current $i_{\alpha s}$ is relevant to both the flux command and the load extent. Thus it is not expected that a higher value of $|\hat{\psi}_r^*|$ always corresponds to a larger magnitude of $i_{\alpha s}$ in the case of adequate load. Similar phenomena are observed in the subsequent experiment.

C. Practical Considerations

1) *Pure Integration of VM*: As mentioned in the introduction, the pure integration can be amended by several techniques, however those techniques may also cause some problems. In this paper, none of those techniques is needed, because the pure integration is stabilized by the correction term $-k^{VM}\varepsilon$ in VM.

2) *Choice of c_1 and c_2* : Generally speaking, the magnitude c_1 should be properly chosen, because large c_1 overwhelms the information of $\tilde{\omega}_r$ in ε_T . However during experiment, it is observed that using of the term $-k^{VM}\varepsilon$ in VM is adequate to limit ε_T around zero (see Fig. 1). Taking into account the fact that the Lyapunov stability analysis may give conservative results, c_1 and c_2 are chosen to be 0 to simplify the design. The experiment results show that accurate estimations of parameters are still achieved, especially of the rotor resistance.

3) *Hybrid Algorithm for Improving Robustness*: To make the adaptation process of $\hat{\alpha}$ more robust, we alter the adapta-

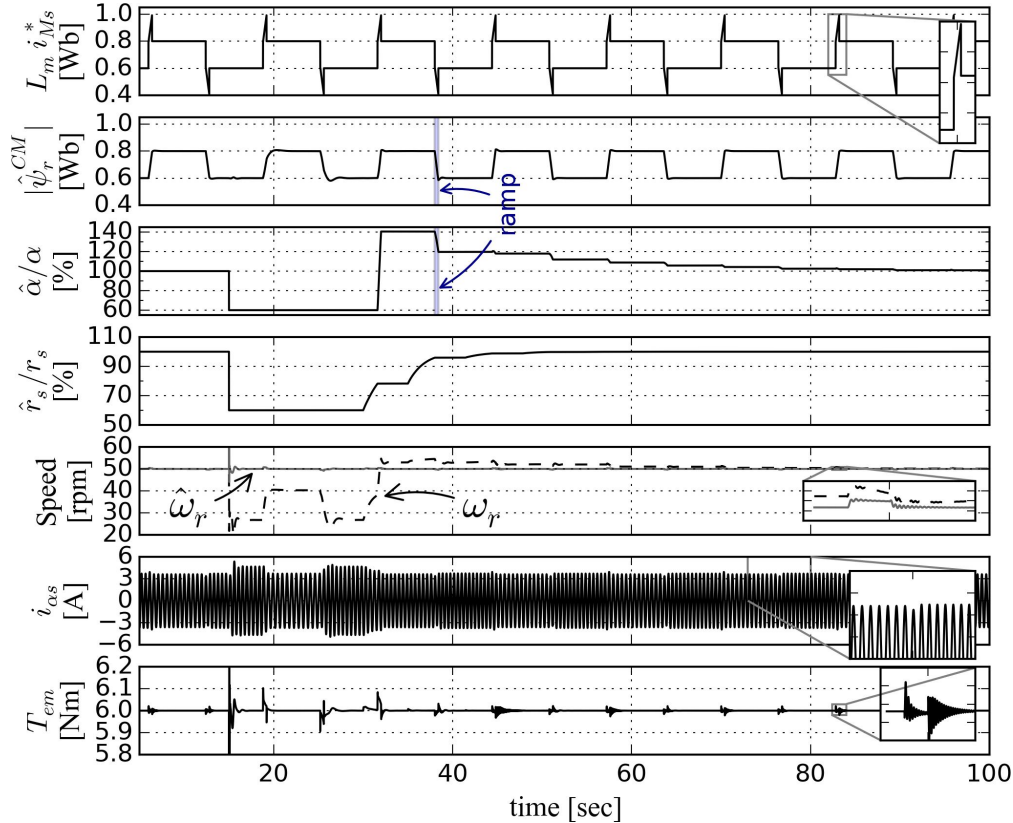
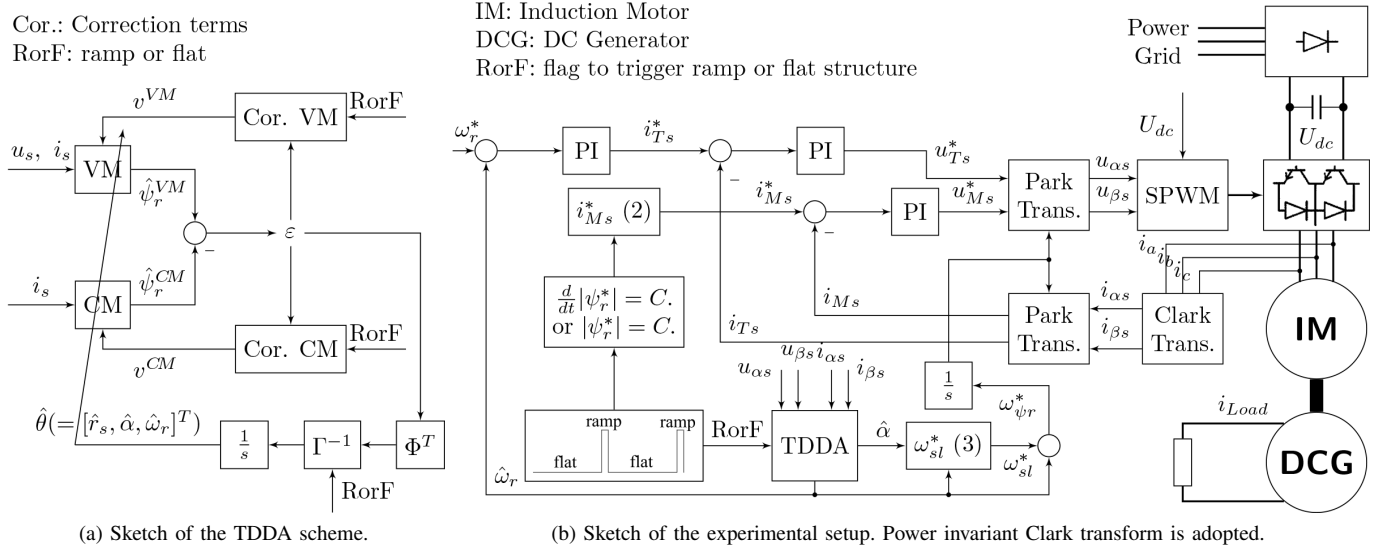


Fig. 3. Simulated results of the resistances adaptation in speed sensorless system at 50 rpm with constant load torque of 6 Nm. \hat{r}_s and $\hat{\alpha}$ are set to 60% of the actual values at $t = 15$ s.

tion rule for $\hat{\alpha}$ into a discrete fashion according to the hybrid algorithm described in [30, Chap. 8].

$$\begin{aligned} \hat{\alpha}(t_{i+1}) = & \hat{\alpha}(t_i) + \gamma_\alpha \int_{t_a}^{t_b} \left[-L_r \hat{i}_{\alpha r} \varepsilon_\alpha - L_r \hat{i}_{\beta r} \varepsilon_\beta \right] dt \\ & + \gamma_\alpha \int_{t_c}^{t_{i+1}} \left[-L_r \hat{i}_{\alpha r} \varepsilon_\alpha - L_r \hat{i}_{\beta r} \varepsilon_\beta \right] dt \end{aligned} \quad (26)$$

where the integral span is actually one period of ramp structure, and the meanings of t_a , t_b and t_c are delineated in Fig. 4. As a result, the possible torque ripple caused by oscillation of $\hat{\alpha}$ adaptation is avoided.

4) Delayed Stator Resistance Adaptation: Due to transient process, it is not guaranteed that the modulus of estimated rotor flux is constant during the whole period of the flat

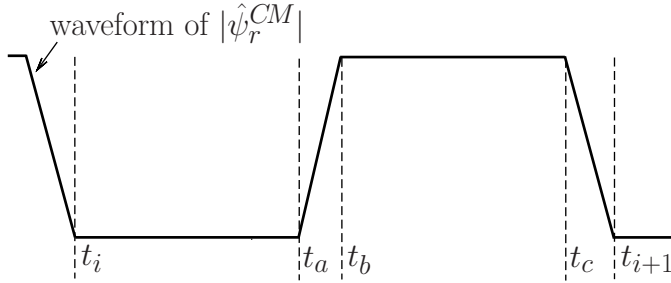


Fig. 4. Graphic illustration for the hybrid algorithm. The integral span of each update of $\hat{\alpha}$ equals to one period of ramp structure.

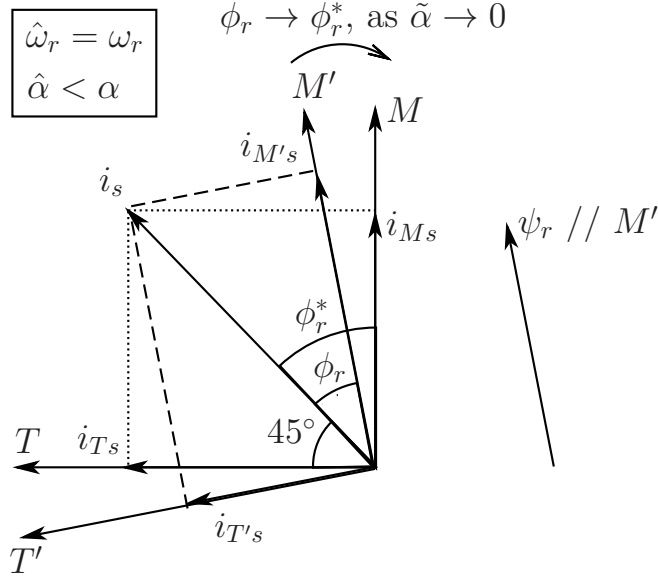


Fig. 5. Vector plot of i_s decomposition when $\hat{\alpha} < \alpha$, where ϕ_r and ϕ_r^* are the actual and controlled rotor impedance angle respectively. Note in the case of $\hat{\alpha} < \alpha$ the actual magnetizing current i_M' is larger than the measured one i_{Ms} , which may lead to saturation of the magnetic circuit.

structure. Hence, the duty ratio of \hat{r}_s adaptation is introduced so that \hat{r}_s adaptation is delayed turning on after $t_{DoF} \times \vartheta_{duty}$ seconds, where t_{DoF} is the duration of the flat structure, and $0 \leq \vartheta_{duty} \leq 1$ is the duty ratio (see Table II).

5) *Influence on Field Orientation with Detuned $\hat{\alpha}$* : It is affirmative that the stator current command and the synchronous frequency command can be tracked, i.e. $i_s = i_s^*$ and $\omega_{\psi r} = \omega_{\psi r}^*$ in speed sensorless system, and if $\hat{\alpha}$ and $\hat{\omega}_r$ are used to calculate the synchronous speed $\omega_{\psi r}^*$, then we have at steady state

$$\omega_{\psi r} = \omega_r + \alpha \frac{i_{T'} s}{i_{M'} s} = \hat{\omega}_r + \hat{\alpha} \frac{i_{T'} s}{i_{M'} s} = \omega_{\psi r}^* \quad (27)$$

where M' and T' are axes of the M' - T' frame, M' is aligned with the actual rotor field, and T' axis is 90° lending to M' axis. And it yields

$$\tilde{\omega}_r + \tilde{\alpha} \frac{i_{T'} s}{i_{M'} s} = \omega_r + \alpha \frac{i_{T'} s}{i_{M'} s} - \hat{\omega}_r - \hat{\alpha} \frac{i_{T'} s}{i_{M'} s} = \alpha \left(\frac{i_{T'} s}{i_{M'} s} - \frac{i_{T'} s}{i_{M'} s} \right) \quad (28)$$

from which it implies that if $\tilde{\omega}_r + \tilde{\alpha} \frac{i_{T'} s}{i_{M'} s} \neq 0$, then the M - T frame is bias placed because the controlled rotor impedance

angle ϕ_r^* does not equal to the actual one ϕ_r

$$\begin{aligned} \phi_r^* &= \tan^{-1} (\omega_{sl}^* \hat{\alpha}^{-1}) = \tan^{-1} \left(\frac{i_{T'} s}{i_{M'} s} \right) \\ &\neq \tan^{-1} \left(\frac{i_{T'} s}{i_{M'} s} \right) = \tan^{-1} (\omega_{sl} \alpha^{-1}) = \phi_r \end{aligned} \quad (29)$$

and the formula of the torque T_{em} in such a situation can be deduced as

$$\begin{aligned} T_{em} &= n_{pp} \frac{L_m}{L_r} \left[i_{T'} s \psi_{Mr}^* + \frac{1}{1 + \omega_{sl}^2 \alpha^{-2}} \left(\frac{i_{T'} s}{i_{M'} s} - \frac{i_{T'} s}{i_{M'} s} \right) \right. \\ &\quad \times \left. \left(\frac{i_{T'} s}{i_{M'} s} \frac{i_{T'} s}{i_{M'} s} - 1 \right) i_{M'} s \psi_{Mr}^* \right] \end{aligned} \quad (30)$$

where the M' axis of M' - T' frame is aligned with the actual rotor field, and T' axis is 90° lending to M' axis.

The above results can be taken advantage of to evaluate the accuracy of $\hat{\alpha}$. putting $\frac{i_{T'} s}{i_{M'} s} = 1$ it yields

$$\begin{aligned} T_{em} &= n_{pp} \frac{L_m}{L_r} \left[i_{T'} s \psi_{Mr}^* - \frac{1}{1 + \omega_{sl}^2 \alpha^{-2}} \left(\frac{i_{T'} s}{i_{M'} s} - 1 \right)^2 \right. \\ &\quad \times \left. i_{M'} s \psi_{Mr}^* \right] \end{aligned} \quad (31)$$

where it is noted the actual torque has a maximum which equals to the torque command $T_{em}^* = n_{pp} L_m L_r^{-1} i_{T'} s \psi_{Mr}^*$ at $i_{T'} s / i_{M'} s = 1$ (i.e. $\hat{\alpha} = \alpha$ if $\hat{\omega}_r = \omega_r$). Refer to Fig. 5 to get a graphical interpretation. Note that the above deductions are valid in the core saturation region as well.

D. Experiment Results

Fig. 6, Fig. 7 and Fig. 8 show the resistances identification results at low speed (around 1.67 Hz excitation). Fig. 6, Fig. 7 and Fig. 8 correspond to cases of under-estimated, over-estimated and excessive over-estimated of resistances respectively. The estimated speed $\hat{\omega}_r$ is always kept around 50 rpm which matches the speed command. Since the resistances are set to incorrect values intentionally, the actual speed ω_r deviates from $\hat{\omega}_r$ at the beginning. The adaptation of resistances is turned on at $t = 20$ s. It is observed that $\hat{\alpha}$ may tend to some incorrect value before \hat{r}_s converges. The actual speed ω_r finally tends to the estimated speed as resistances converge, and speed ripples caused by ramp flux command are evident during low speed operation. Particularly, in Fig. 8 when \hat{r}_s is far larger than the nominal value, the system oscillates at a certain degree. And the adaptation of \hat{r}_s and $\hat{\alpha}$ stabilizes the system. Analogue instability phenomena are reported in [3]. Thus, the whole scheme is believed to be robust to disturbance. It is confirmed that stator resistance is crucial for system stability at low speed, and both stator and rotor resistance have great impact on the controlled speed accuracy.

To evaluate the accuracy of the estimated rotor resistance, a *torque command experiment* is designed. In such an evaluation purpose experiment, sensed speed is used in control, so that the value of α^* is the only source for affecting the orientation accuracy of the rotor field, which further influences the torque capability of the motor. The torque current command $i_{T'} s$ is

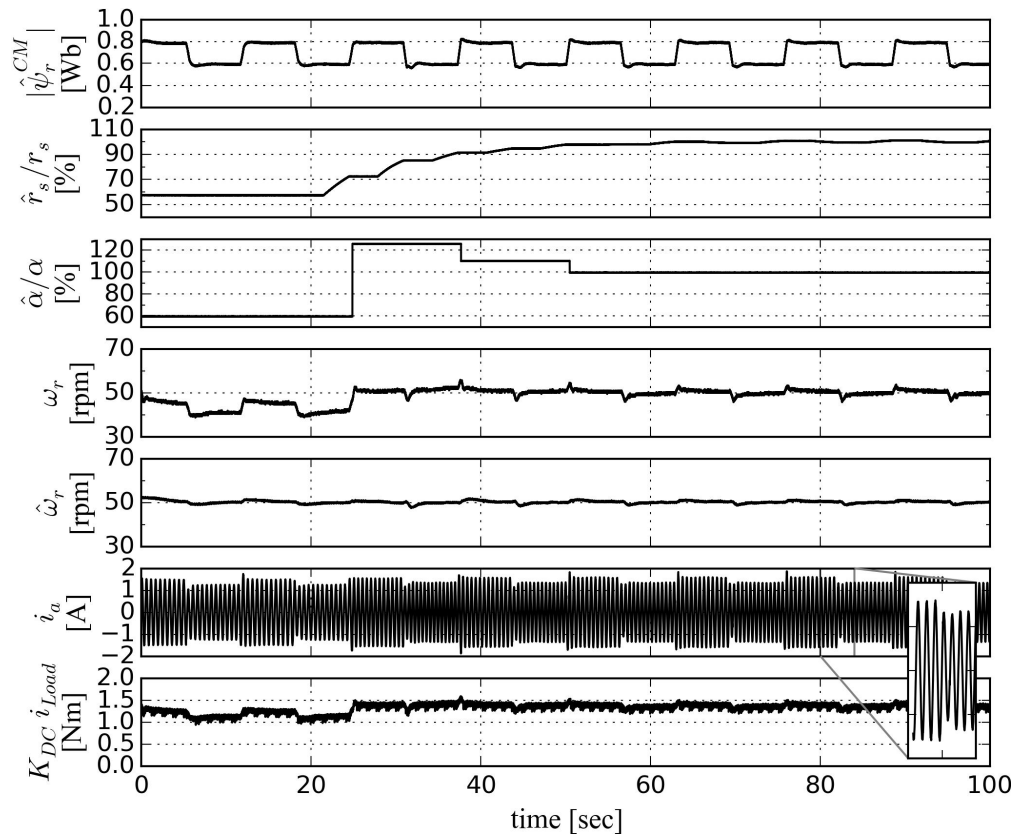


Fig. 6. Experiment results for online adaptation of \hat{r}_s , $\hat{\alpha}$, $\hat{\omega}_r$ at 50 rpm. $\hat{r}_s|_{t=0} = 57\%r_s$, $\hat{\alpha}|_{t=0} = 60\%\alpha$.

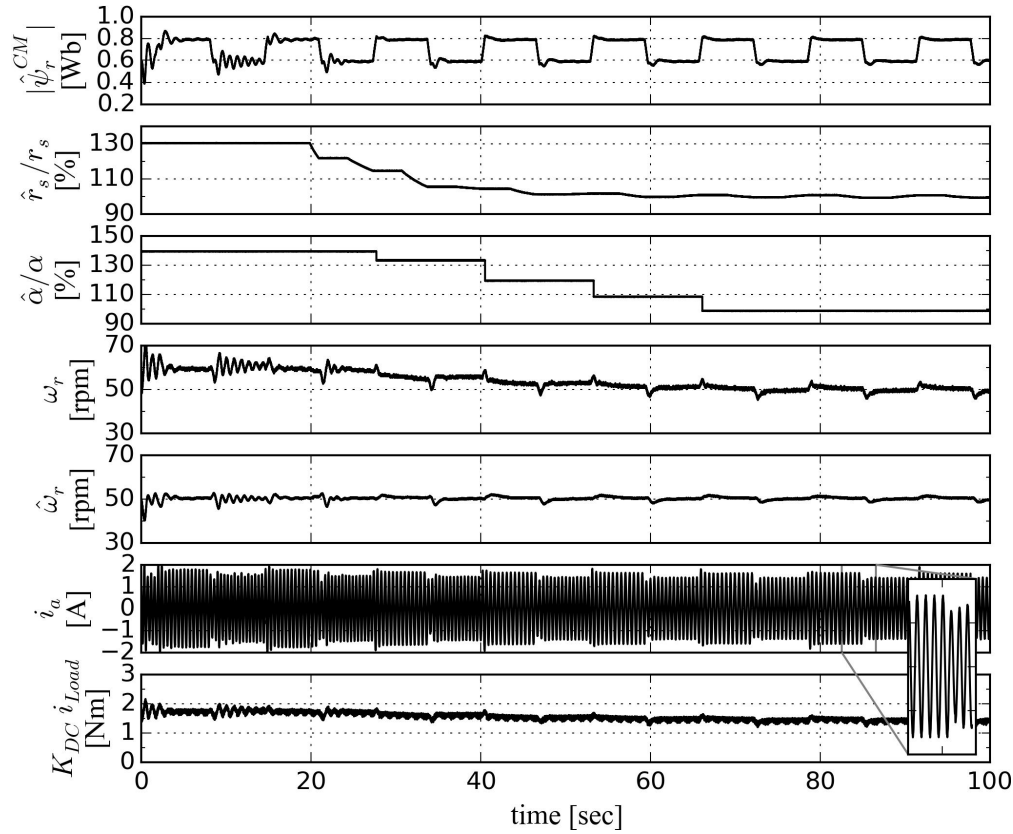


Fig. 7. Experiment results for online adaptation of \hat{r}_s , $\hat{\alpha}$, $\hat{\omega}_r$ at 50 rpm. $\hat{r}_s|_{t=0} = 133\%r_s$, $\hat{\alpha}|_{t=0} = 140\%\alpha$.

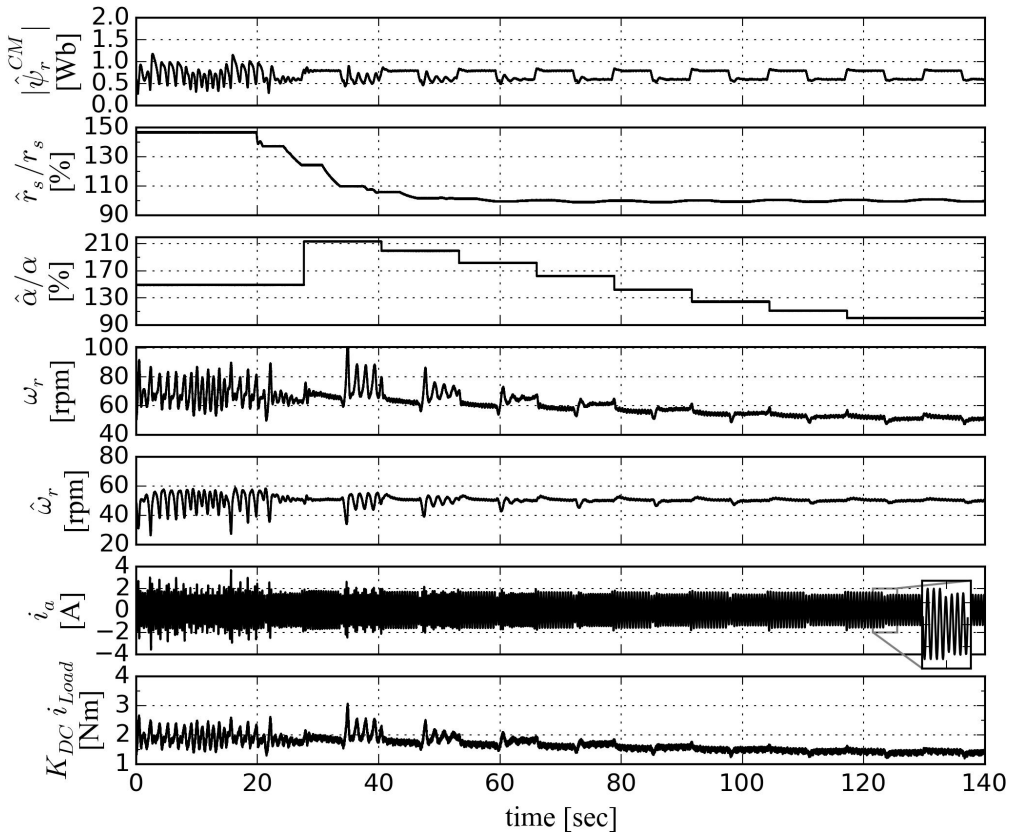


Fig. 8. Experiment results for online adaptation of \hat{r}_s , $\hat{\alpha}$, $\hat{\omega}_r$ at 50 rpm. $\hat{r}_s|_{t=0} = 147\%r_s$, $\hat{\alpha}|_{t=0} = 150\%\alpha$.

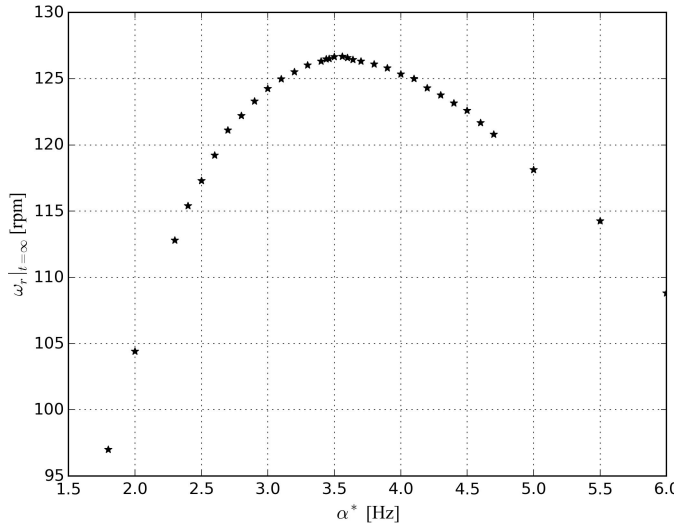


Fig. 9. Experiment results for evaluating the accuracy of different values of α^* . Torque current command $i_{T_s}^*$ is equal to $i_{M_s}^*$, and kept invariant throughout the experiment.

equal to $i_{M_s}^*$ and kept invariant throughout, and the magnetic excitation current of the DC generator is kept invariant as well. It is then reasonable to evaluate the accuracy of different values of α^* by observing the steady state rotor speed $\omega_r|_{t=\infty}$. Since ω_r is proportional to the load torque produced by the DC generator, the value of $\omega_r|_{t=\infty}$ is a clear index for the mechanical torque produced by the motor. The steady state

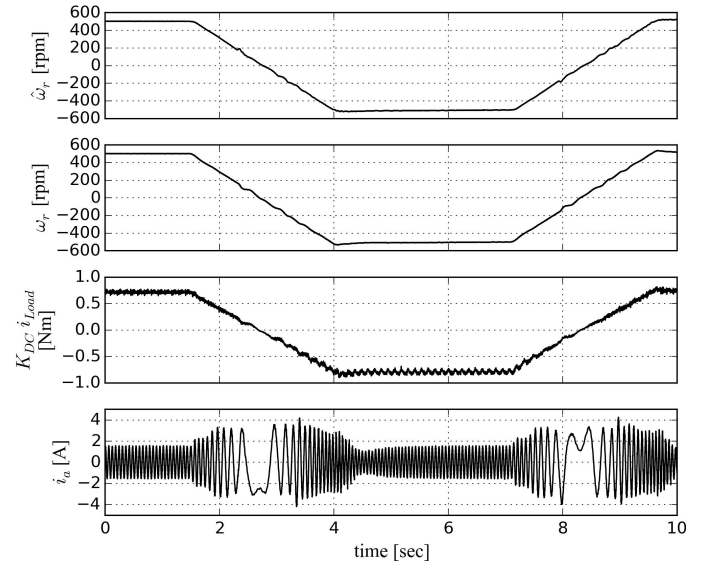


Fig. 10. Reversing test of the speed command between -500 rpm and 500 rpm.

rotor speed $\omega_r|_{t=\infty}$ reaches a maximum when α^* equals to the actual value. The $\omega_r|_{t=\infty}$ to α^* plot is depicted in Fig. 9. The theory support of this experiment comes from (31). The results of this experiment further confirms the feasibility of the proposed scheme, and accurate value of rotor resistance is identified.

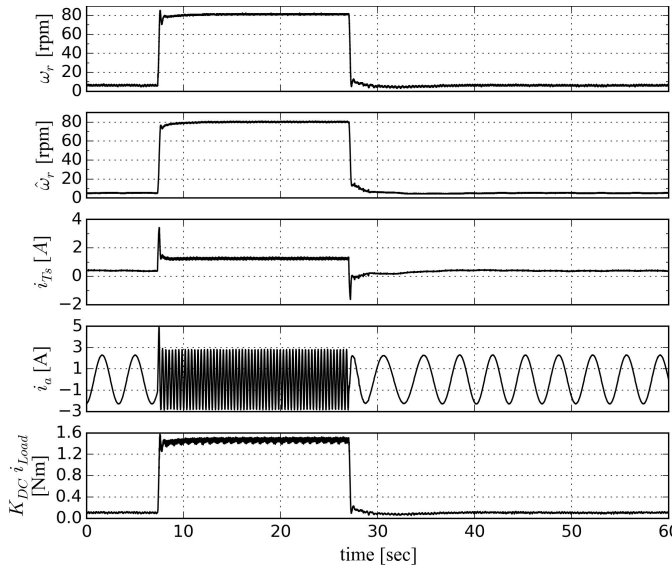


Fig. 11. Step speed command test of the speed command between 5 rpm and 80 rpm.

Fig 10 gives the waveforms of ω_r , $\hat{\omega}_r$ and phase current i_a during motor reversing. The speed command is set to 500 rpm, then goes down to -500 rpm and finally back to 500 rpm. It can be concluded that the system performance is available during zero crossing operation. During the experiment, it is discovered that a smaller value of k^{VM} (or equivalently a larger $\gamma_{\omega r}$) results in better dynamic performance during zero speed crossing where the sensitivity of ε with respect to $\hat{\omega}_r$ becomes low. In addition, it is observed that the load torque (i.e. $K_{DC}i_{Load}$) oscillates at two times the frequency of current and higher frequency. The former is caused by the unbalanced current metering scaling, and the latter is incurred by the open rotor slots.

Fig 11 presents the system response to speed step change during extremely low speed operation. The speed command is initially 5 rpm, and steps to 80 rpm and then steps back to 5 rpm. The results show that the system preserves good performance in the extremely low speed operation. Thus, the above results verify the effectiveness of the proposed speed estimator.

IV. CONCLUSION

This paper addresses the method for stator and rotor resistance identification in speed sensorless induction motor drives. The pure integration problem of the voltage model is well handled, hence computation burden is lessened. The proposed robust adaptive flux observer is derived with rigorous stability analysis, where input-to-state stability is needed to discuss the performance of the observer exposed to disturbances. Main theoretical difficulties are overcome by introducing 1) the variable structure in adaptation rules and 2) the correction terms in the voltage model and the current model.

- 1) The variable structure in adaptation rules relaxes the persistent excitation condition to order two, while the third estimated parameter error is regarded as disturbance. The idea is inspired by the concept of time division multiplexing,

and is feasible due to the decoupled identifiability of stator resistance with respect to other two parameters. In addition, to distinguish the rotor time constant from the rotor speed, instead of injecting an extra sinusoidal flux modulus, the ramp flux modulus command is proposed, which is believed to be more efficient.

- 2) The correction terms that are functions of the mismatch between voltage model and current model, help to resist disturbance and in the meantime to stabilize the voltage model. In theory, the complete decoupled identifiability of stator resistance is obtained by further incorporating sliding mode control into the correction terms.

The feasibility of the proposed observer and the accuracy of the estimated parameters are verified by simulation and experimental results. In practice, hybrid algorithm is incorporated to enhance the robustness of the rotor resistance identification. To evaluate the accuracy of the unavailable rotor resistance, a *torque command experiment* is designed, where the output torque of the motor reaches its maximum only when estimated rotor resistance matches the actual one. The further researches should incorporate dynamic nonlinear control to reduce the torque ripple caused by the varying flux modulus command, and take the current dependency of the inductances into account.

APPENDIX A CONVERGENCE ANALYSIS OF PARAMETERS

A. Flat Structure

The expected results of the observer in flat structure are that $\tilde{i}_s \rightarrow 0$, as $t \rightarrow \infty$. In this sub-section, \hat{i}_{Mr} is assumed to be zero due to $|\psi_r^*| = \text{Const.}$, thus the derivative of Lyapunov function \dot{V} in (24) for the system (21) becomes

$$\dot{V} = x^T Ax + x^T \left(\begin{bmatrix} 0 \\ 0 \\ 0 \\ \hat{\psi}_{Mr}^{CM} \end{bmatrix} \tilde{\omega}_r - \begin{bmatrix} 0 \\ L_r \hat{i}_{Tr} \\ 0 \\ L_r \hat{i}_{Tr} \end{bmatrix} \tilde{\alpha} - \begin{bmatrix} 0 \\ c_1 \text{sgn}(\varepsilon_T) \\ 0 \\ c_2 \text{sgn}(e_T) \end{bmatrix} \right) \quad (32)$$

If the magnitudes c_1 and c_2 satisfy (sliding mode surface is chosen as $[\varepsilon_T, e_T]^T = 0$)

$$\begin{cases} c_1 > |L_r \hat{i}_{Tr} \tilde{\alpha}| \\ c_2 > |\hat{\psi}_{Mr}^{CM} \tilde{\omega}_r - L_r \hat{i}_{Tr} \tilde{\alpha}| \end{cases} \quad (33)$$

Then it arrives at

$$\dot{V} \leq x^T Ax$$

According to Barbalat's Lemma (see [31]) it yields that $x \rightarrow 0$ as $t \rightarrow \infty$, and z^f is bounded. To derive the asymptotical stability of \tilde{i}_s , choose another auxiliary function for the M -axis subsystem

$$W^M(\varepsilon_M, e_M, \tilde{i}_s) = \begin{bmatrix} \varepsilon_M \\ e_M \end{bmatrix}^T \begin{bmatrix} L_r L_m^{-1} i_{Ms} \\ 0 \end{bmatrix} \tilde{i}_s \quad (34)$$

the derivative of which follows

$$\begin{aligned}\dot{W}^M &= \dot{\varepsilon}_M (L_r L_m^{-1} i_{Ms}) \tilde{r}_s + \varepsilon_M (L_r L_m^{-1} \dot{i}_{Ms}) \tilde{r}_s \\ &\quad + \varepsilon_M (L_r L_m^{-1} i_{Ms}) \dot{\tilde{r}}_s \\ &= \{- (k^{VM} + \hat{\alpha}) \varepsilon_M + (\omega_{\psi r} - \hat{\omega}_r) \varepsilon_T - \alpha \varepsilon_M \\ &\quad + \omega_r e_T + (L_r L_m^{-1} i_{Ms}) \tilde{r}_s\} (L_r L_m^{-1} i_{Ms}) \tilde{r}_s \\ &\quad + \varepsilon_M (L_r L_m^{-1} i_{Ms}) \tilde{r}_s + \varepsilon_M (L_r L_m^{-1} i_{Ms}) \dot{\tilde{r}}_s\end{aligned}\quad (35)$$

which is a positive definite function if $\dot{V} = 0$ (i.e. $x = 0$) and $i_{Ms} \neq 0$, and by Matrosov's Theorem [32, p.62] it concludes the asymptotical stability of \tilde{r}_s .

Remark: According to the discussion in Sec. III-C5. The disturbance in the dynamics of e_T is caused by biased field orientation, since at steady state we have

$$\begin{aligned}\left| \hat{\psi}_{Mr}^{CM} \tilde{\omega}_r - L_r \hat{i}_{Tr} \tilde{\alpha} \right| &= \hat{\psi}_{Mr}^{CM} \left| \tilde{\omega}_r + \tilde{\alpha} \frac{i_{Ts}^*}{i_{Ms}^*} \right| \\ &= \hat{\psi}_{Mr}^{CM} \alpha \left| \frac{i_{Ts}^*}{i_{Ms}^*} - \frac{i_{T's}}{i_{M'}^*} \right|\end{aligned}\quad (36)$$

B. Ramp Structure

The expected results of the observer in ramp structure are that estimated parameter errors $z^r \rightarrow 0$, as $t \rightarrow \infty$ if $\tilde{r}_s = 0$. Assume that \tilde{r}_s has converged to zero, i.e. the disturbance $w^r = \tilde{r}_s = 0$, thus the dynamics (25) becomes

$$\begin{cases} \dot{x} = Ax + B\Psi z^r \\ \varepsilon^{MT} = Hx \end{cases}\quad (37)$$

in which $\Psi = \begin{bmatrix} -L_r \hat{i}_r^{MT} & J \hat{\psi}_r^{CM MT} \end{bmatrix}$, $B = \begin{bmatrix} I \\ I \end{bmatrix}$, $H = \begin{bmatrix} I & 0 \end{bmatrix}$, and the triple (H, A, B) is strictly positive real, so that by multivariable LKY Lemma (see e.g. [33, p.79]) there exists a symmetric positive definite matrix P satisfying

$$\begin{aligned}PA + A^T P &= -Q \\ PB &= H^T\end{aligned}\quad (38)$$

where Q is a symmetric positive definite matrix. As a result, put $\Gamma^r = \text{diag}(\gamma_2, \gamma_3)$, and the adaptation rule driven by partial states (from 2nd, 3rd equations in (6))

$$\dot{z}^r = -\Gamma^{r-1} \Psi^T \varepsilon^{MT}\quad (39)$$

guarantees the asymptotical stability of x , which is apparent by introducing a Lyapunov function $U : \mathbb{R}^4 \times \mathbb{R}^2 \rightarrow \mathbb{R}$

$$U(x, z^r) = x^T P x + z^{rT} \Gamma^r z^r\quad (40)$$

whose derivative follows as

$$\begin{aligned}\dot{U} &= x^T (A^T P + PA) x + (x^T P B \Psi z^r + z^{rT} \Psi^T B^T P x) \\ &\quad + (z^{rT} \Gamma^r z^r + \dot{z}^{rT} \Gamma^r z^r) \\ &= -x^T Q x + (x^T H^T \Psi z^r + z^{rT} \Psi^T H x) \\ &\quad + (z^{rT} \Gamma^r \dot{z}^r + \dot{z}^{rT} \Gamma^r z^r) \\ &\stackrel{(39)}{=} -x^T Q x\end{aligned}\quad (41)$$

Furthermore, consider a set \mathcal{E} excluding the origin

$$\begin{aligned}\mathcal{E} &\stackrel{\Delta}{=} \{(x, z^r) : \dot{U}(x, z^r) = 0, z^r \neq 0\} \\ &= \{(x, z^r) : x = 0, z^r \neq 0\}\end{aligned}\quad (42)$$

and a second auxiliary function $W : \mathbb{R}_{>0} \times \mathbb{R}^4 \times \mathbb{R}^2 \rightarrow \mathbb{R}$

$$W(t, x, z^r) = (Hx)^T \Psi z^r\quad (43)$$

which in fact is related to the derivative of $z^{rT} z^r$, and the derivative of W along (37) is

$$\dot{W} = (H A x + H B \Psi z^r)^T \Psi z^r + x^T H^T \dot{\Psi} z^r + x^T H^T \Psi \dot{z}^r\quad (44)$$

And if $\Psi^T \Psi$ is positive definite (as in (12c)) in the set \mathcal{E} , by Matrosov's Theorem it yields that z^r is asymptotically stable.

Remark—The ramp flux modulus command: From the lemma Upper Bound for the Escape Time of a Solution [32, p.61], the duration of (x, z^r) staying in \mathcal{E} is inversely proportional to \dot{W} . Thus a persistent and strong excitation in regressive matrix Ψ leads to faster convergent rate of parameter estimations (towards $(0, 0)$). Since the positive definiteness of $\Psi^T \Psi$ becomes lost periodically when a sinusoidal flux modulus command is injected, the ramp flux modulus command is believed to be more efficient by keeping $\hat{i}_{Mr} = \text{Const.}$

REFERENCES

- [1] Kamarudin B, Nordin D.W, Novotny D.S, Zinger. The influence of motor parameter deviations in feedforward field orientation drive systems. *Industry Applications, IEEE Transactions on*, IA-21(4):1009–1015, July 1985.
- [2] Hirokazu Tajima and Yoichi Hori. Speed sensorless field-orientation control of the induction machine. *Industry Applications, IEEE Transactions on*, 29(1):175–180, 1993.
- [3] Lennart Harnefors. Instability phenomena and remedies in sensorless indirect field oriented control. *Power Electronics, IEEE Transactions on*, 15(4):733–743, Jul 2000.
- [4] H.A. Toliyat, E. Levi, and M. Raina. A review of rfo induction motor parameter estimation techniques. *Energy Conversion, IEEE Transactions on*, 18(2):271–283, June 2003.
- [5] C.M. Verrelli, A. Savoia, M. Mengoni, R. Marino, P. Tomei, and L. Zarri. On-line identification of winding resistances and load torque in induction machines. *Control Systems Technology, IEEE Transactions on*, 22(4):1629–1637, July 2014.
- [6] K. Kubota and K. Matsuse. Speed sensorless field-oriented control of induction motor with rotor resistance adaptation. *Industry Applications, IEEE Transactions on*, 30(5):1219–1224, Sep 1994.
- [7] C. Ilas, G. Griva, and F. Profumo. Wide range speed sensorless induction motor drives with rotor resistance adaptation. In *Power Electronics, Drives and Energy Systems for Industrial Growth, 1996., Proceedings of the 1996 International Conference on*, volume 1, pages 211–215 vol.1, Jan 1996.
- [8] H. Hofmann and S. R. Sanders. Speed-sensorless vector torque control of induction machines using a two-time-scale approach. In *IEEE Trans. Ind. Applicat.*, pages 169–177, 1998.
- [9] Hirokazu Tajima, Giuseppe Guidi, and Hidetoshi Umida. Consideration about problems and solutions of speed estimation method and parameter tuning for speed-sensorless vector control of induction motor drives. *Industry Applications, IEEE Transactions on*, 38(5):1282–1289, 2002.
- [10] S. Suwankawin and S. Sangwongwanich. Design strategy of an adaptive full-order observer for speed-sensorless induction-motor drives-tracking performance and stabilization. *IEEE Transactions on Industrial Electronics*, 53(1):96–119, Feb 2005.
- [11] M. S. Zaky. Stability analysis of speed and stator resistance estimators for sensorless induction motor drives. *IEEE Transactions on Industrial Electronics*, 59(2):858–870, Feb 2012.
- [12] Riccardo Marino, P. Tomei, and CM Verrelli. Adaptive control for speed-sensorless induction motors with uncertain load torque and rotor resistance. *International Journal of Adaptive Control and Signal Processing*, 19(9):661–685, 2005.
- [13] Pavel Vaclavek, Peter Blaha, and Ivo Herman. Ac drive observability analysis. *Industrial Electronics, IEEE Transactions on*, 60(8):3047–3059, 2013.
- [14] Kan Akatsu and Atsuo Kawamura. Sensorless very low-speed and zero-speed estimations with online rotor resistance estimation of induction motor without signal injection. *Industry Applications, IEEE Transactions on*, 36(3):764–771, 2000.

- [15] Riccardo Marino, Sergei Peresada, and Patrizio Tomei. On-line stator and rotor resistance estimation for induction motors. *Control Systems Technology, IEEE Transactions on*, 8(3):570–579, 2000.
- [16] Seok Ho Jeon, Kwang Kyo Oh, and Jin Young Choi. Flux observer with online tuning of stator and rotor resistances for induction motors. *Industrial Electronics, IEEE Transactions on*, 49(3):653–664, 2002.
- [17] T Abbasian, FR Salmasi, and MJ Yazdanpanah. Stability analysis of sensorless im based on adaptive feedback linearization control with unknown stator and rotor resistances. In *Industry Applications Conference, 2005. Fourtieth IAS Annual Meeting. Conference Record of the 2005*, volume 2, pages 985–992. IEEE, 2005.
- [18] Riccardo Marino, Patrizio Tomei, and Cristiano Maria Verrelli. Tracking control for sensorless induction motors with uncertain load torque and resistances. In *Nonlinear Control Systems*, pages 771–776, 2010.
- [19] Riccardo Marino, Patrizio Tomei, and Cristiano Maria Verrelli. A new flux observer for induction motors with on-line identification of load torque and resistances. In *18th IFAC World Congress, Milano, Italy*, volume 18, pages 6172–6177, 2011.
- [20] Fabrice Jadot, Francois Malrait, Javier Moreno-Valenzuela, and Rodolphe Sepulchre. Adaptive regulation of vector-controlled induction motors. *Control Systems Technology, IEEE Transactions on*, 17(3):646–657, 2009.
- [21] R Marino, P Tomei, and CM Verrelli. Adaptive output feedback tracking control for induction motors with uncertain load torque and resistances. In *Power Electronics Electrical Drives Automation and Motion (SPEEDAM), 2010 International Symposium on*, pages 419–424. IEEE, 2010.
- [22] Riccardo Marino, Tomei Patrizio, and Maria Cristiano Verrelli. Adaptive output feedback control of induction motors. *AC Electric Motors Control: Advanced Design Techniques and Applications*, Wiley Online Library:158–187, 2013.
- [23] Colin Schauder. Adaptive speed identification for vector control of induction motors without rotational transducers. *Industry applications, IEEE Transactions on*, 28(5):1054–1061, 1992.
- [24] Veran Vasic, Slobodan N Vukosavic, and Emil Levi. A stator resistance estimation scheme for speed sensorless rotor flux oriented induction motor drives. *Energy Conversion, IEEE Transactions on*, 18(4):476–483, 2003.
- [25] Lihang Zhao, Jin Huang, He Liu, Bingnan Li, and Wubin Kong. Second-order sliding-mode observer with online parameter identification for sensorless induction motor drives. *Industrial Electronics, IEEE Transactions on*, 61(10):5280–5289, 2014.
- [26] N. R. N. Idris and A. H. M. Yatim. An improved stator flux estimation in steady-state operation for direct torque control of induction machines. *IEEE Transactions on Industry Applications*, 38(1):110–116, Jan 2002.
- [27] Jun Hu and Bin Wu. New integration algorithms for estimating motor flux over a wide speed range. *IEEE Transactions on Power Electronics*, 13(5):969–977, Sep 1998.
- [28] S. Wade, W. Dunnigan, and B. W. Williams. A new method of rotor resistance estimation for vector-controlled induction machines. *IEEE Transactions on Industrial Electronics*, 44(2):247–257, Apr 1997.
- [29] R Marino, Giovanni L Santosuosso, and Patrizio Tomei. Robust adaptive observers for nonlinear systems with bounded disturbances. *Automatic Control, IEEE Transactions on*, 46(6):967–972, 2001.
- [30] Kumpati S Narendra and Anuradha M Annaswamy. *Stable adaptive systems*. Courier Corporation, 1989.
- [31] Riccardo Marino and Patrizio Tomei. *Nonlinear control design: geometric, adaptive and robust*. Prentice Hall International (UK) Ltd., 1996.
- [32] Nicolas Rouche, Patrick Habets, Michel Laloy, and Aleksandr Michajlović Ljapunov. *Stability theory by Liapunov's direct method*, volume 4. Springer, 1977.
- [33] Bernard Brogliato, Rogelio Lozano, Bernhard Maschke, and Olav Egeland. *Dissipative systems analysis and control*. Springer, 2007.



Jiahao Chen was born in Wenzhou, China, in 1991. He received the B.S. degree in electrical engineering from Zhejiang University, Hangzhou, China, in 2014, and is currently a doctoral student at the Institute of Electrical Engineering in Zhejiang University. His research interests include parameter identification and servo control of electric motors.



Jin Huang received the B.Sc. degree in electrical engineering from Zhejiang University, Hangzhou, China, in 1982, and the Ph.D. degree in electrical engineering from the National Polytechnic Institute of Toulouse, Toulouse, France, in 1987. From 1987 to 1994, he was an Associate Professor with the College of Electrical Engineering, Zhejiang University. Since 1994, he has been a Professor at Zhejiang University. His research interests include electrical machine, ac drives, multiphase machine, and motor parameter identification.